Conceptual Design and Preliminary Aerodynamic Analysis of a Tail-Sitter Flying-Wing VTOL UAV

Pushkal Garg

Department of Mechanical Engineering

Indian Institute of Technology Ropar

Contents

Abstract

This report presents the conceptual design, geometric modeling, and preliminary aerodynamic analysis of a tail-sitter vertical takeoff and landing (VTOL) unmanned aerial vehicle (UAV). The project aims to bridge the gap between efficient fixed-wing cruise and rotary-wing hovering capabilities. A tailless flying-wing configuration with twin tractor propulsion was selected to minimize drag and structural complexity. Geometric modeling was performed using OpenVSP, incorporating a blended center body and specific washout to ensure stability. Preliminary aerodynamic analysis using VSPAERO's panel method indicated a zero-lift drag coefficient (C_{D0}) of approximately 0.017, validating the aerodynamic cleanliness of the design. The results demonstrate that the proposed configuration offers a viable solution for missions requiring both endurance and vertical mobility, suitable for further structural optimization and prototype development.

1 Introduction

Vertical takeoff and landing (VTOL) unmanned aerial vehicles (UAVs) have become increasingly important for applications requiring operation in confined or infrastructure-limited environments. While multirotor UAVs provide excellent hover and low-speed maneuverability, their endurance and range are limited by poor aerodynamic efficiency in forward flight. Fixed-wing UAVs, in contrast, offer superior aerodynamic performance but require runways or launch and recovery systems.

Hybrid VTOL concepts aim to combine the advantages of both configurations. Among these, the tail-sitter configuration is particularly attractive due to its mechanical simplicity. By rotating the entire aircraft between vertical and horizontal flight modes, tail-sitters eliminate the need for tilting propulsion systems or auxiliary lifting rotors. However, this simplicity places stringent requirements on aerodynamic efficiency, stability, and control, especially for tailless configurations.

This report presents the conceptual design and preliminary aerodynamic analysis of a tail-sitter UAV based on a flying-wing configuration. The geometry was developed parametrically using OpenVSP, followed by preliminary aerodynamic evaluation using the VSPAERO solver. The primary objective is to assess the feasibility of the proposed configuration at the conceptual design stage and establish a foundation for further structural and high-fidelity aerodynamic studies.

2 Mission Requirements and Design Objectives

2.1 Primary Objectives

- **VTOL Capability:** The vehicle must be capable of taking off and landing vertically from unprepared terrain, utilizing a tail-sitter configuration to minimize mechanical complexity.
- **Efficient Cruise:** The platform must achieve efficient forward-flight performance at low subsonic speeds, surpassing the endurance of comparable multi-rotor systems.
- **Structural Simplicity:** The design should minimize moving parts (e.g., no tilting mechanisms) to ensure robustness and suitability for lightweight manufacturing techniques such as composite molding or foam cutting.

- **Control Authority:** The design must provide adequate control authority in both hover (via differential thrust and slipstream effects) and forward flight (via aerodynamic surfaces) without conventional tail surfaces.

2.2 Performance constraints

A representative cruise condition of approximately **100 km/h** at sea level was selected for aerodynamic evaluation. The design prioritizes low drag, sufficient internal volume for avionics and payload, and compatibility with student-level numerical analysis tools.

3 Configuration Selection

Several VTOL configurations were evaluated, including tilt-wings, separate lift-thrust configurations, and tail-sitters. A **tailless flying-wing tail-sitter** was selected for the following reasons:

1. **Aerodynamic Efficiency:** The flying wing maximizes the lifting surface area relative to wetted area, reducing parasite drag.
2. **Structural Efficiency:** The absence of a long fuselage tail boom reduces bending moments and overall structural weight.
3. **Mechanization:** Unlike tilt-rotors, the motors are rigidly mounted. This reduces failure points and simplifies the autopilot mixing logic.

Twin wing-mounted tractor propellers were chosen to provide symmetric thrust. This arrangement allows for differential thrust to control yaw in hover and roll in forward flight, while also ensuring the control surfaces (elevons) remain in the propeller slipstream for effectiveness at zero forward airspeed.

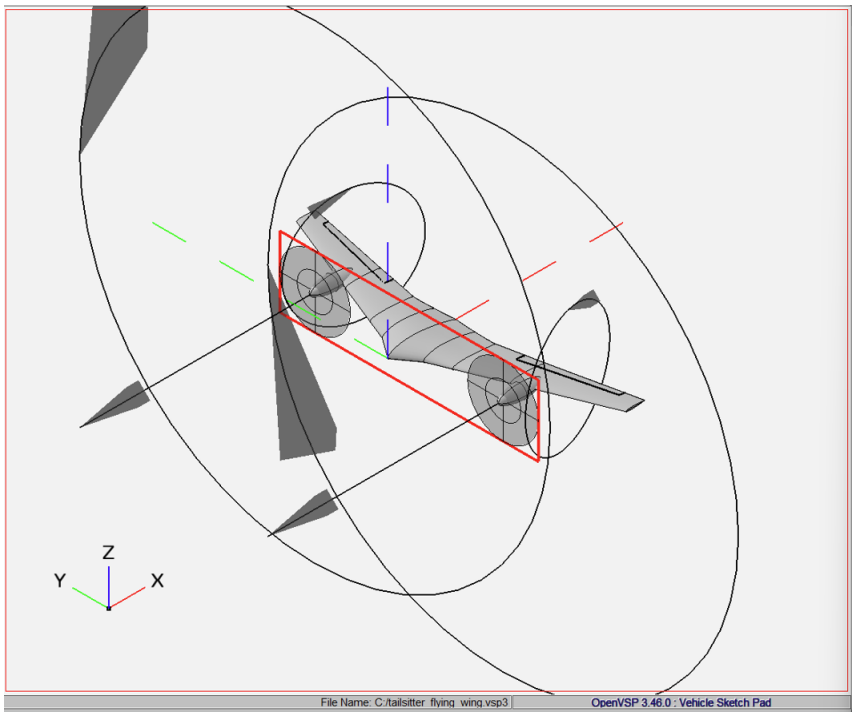

Figure 1: Final OpenVSP geometry of the tail-sitter UAV with twin tractor propulsion.

4 Wing Geometry Design

The wing is the primary lifting surface and the most critical component of the design. Its geometry was iteratively refined in OpenVSP.

4.1 Planform Selection

The wing was designed as a moderately high aspect-ratio flying wing.

- **Aspect Ratio ($\approx$ 9):** A higher aspect ratio reduces induced drag, which is the dominant drag component during the low-speed transition phase and loiter.
- **Sweep:** Moderate leading-edge sweep was applied. This improves longitudinal stability by shifting the aerodynamic center rearward, allowing for a more flexible center of gravity (CG) placement.
- **Taper:** A taper ratio of less than 1.0 was applied to approximate an elliptical lift distribution, thereby minimizing induced drag and reducing the structural weight of the outboard wing sections.

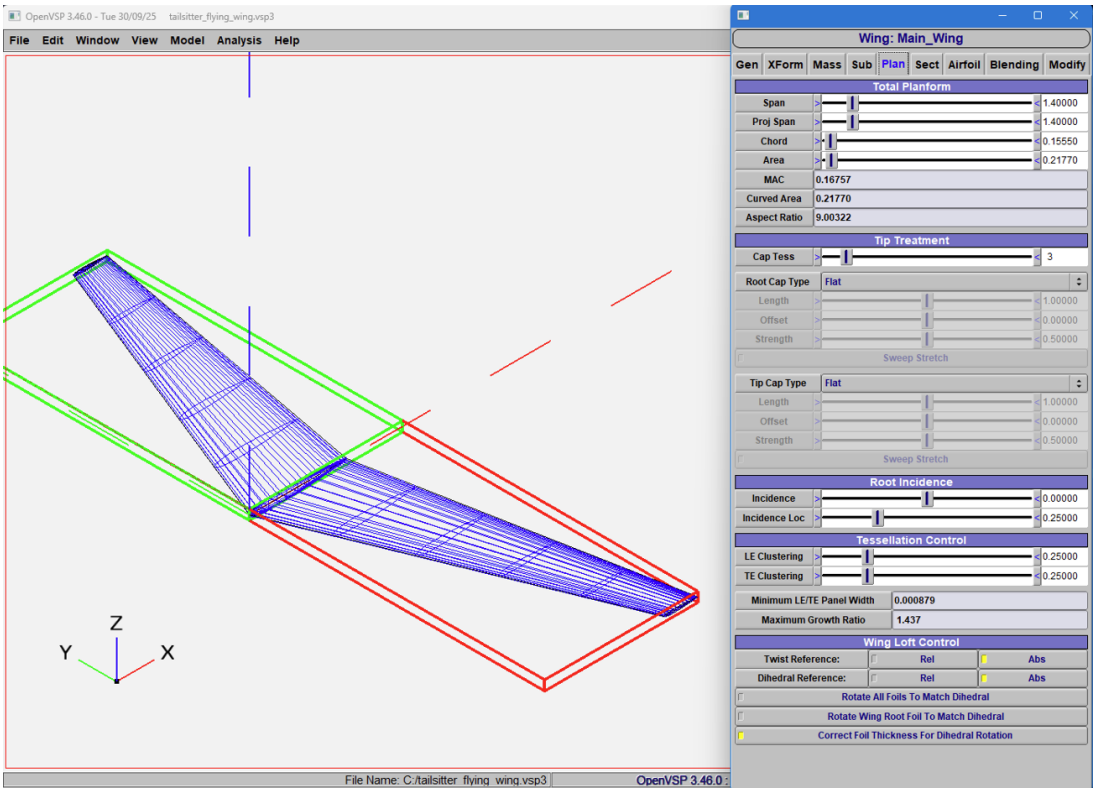

Figure 2: Wing planform definition in OpenVSP showing span, aspect ratio, sweep, and taper.

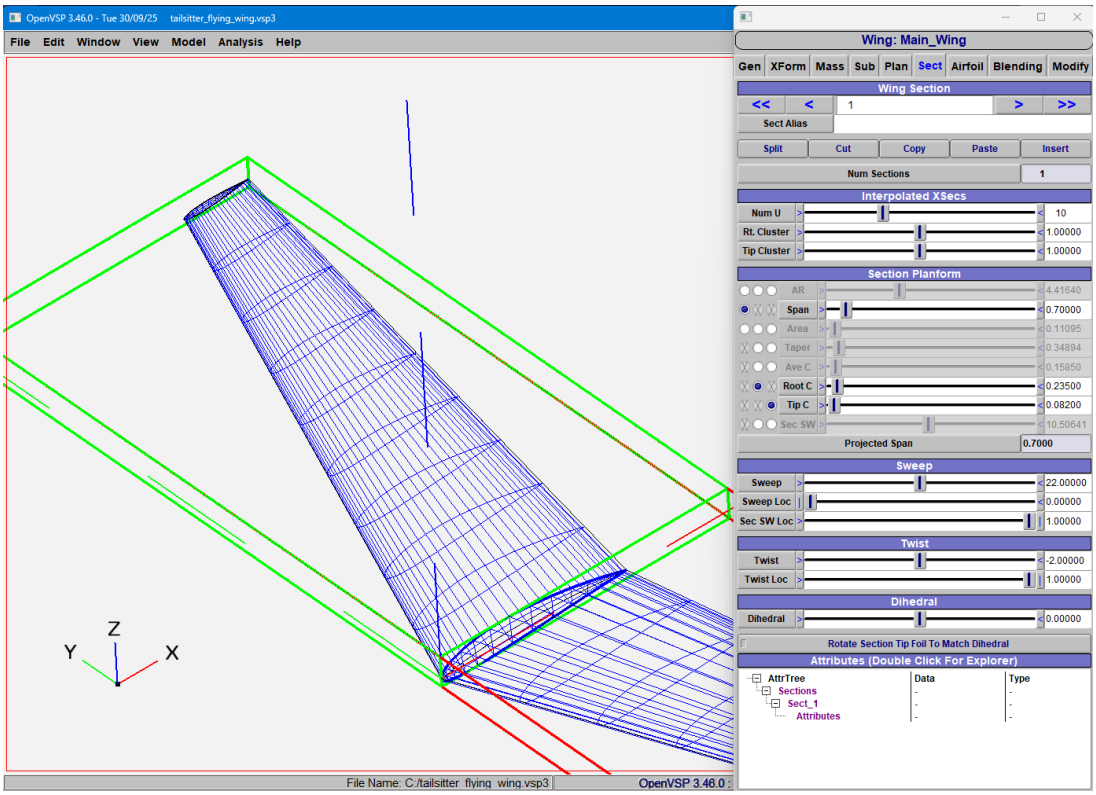

Figure 3: Wing planform definition in OpenVSP showing Root Chord and Tip Chord

4.2 Airfoil Selection

To balance conflicting requirements between the root structural depth and tip stall characteristics, aerodynamic lofting was used between two distinct airfoils:

Table 1: Airfoil Selection and Rationale

Location	Airfoil	Rationale
Root	NACA 4415	15% thickness provides volume for spars and batteries; high $C_{L,max}$ for lift.
Tip	NACA 0012	12% thickness; Symmetric section ensures zero pitching moment at the tips.

Airfoil selection was driven by the need to provide high lift capability at low Reynolds numbers while maintaining acceptable pitching moment characteristics and structural stiffness. At the wing root, a NACA 4415 airfoil with a thickness-to-chord ratio of 15% was selected. The cambered profile provides enhanced lift at moderate angles of attack, which is beneficial during transition and forward flight, while the increased thickness allows space for internal spars and avionics.

At the wing tip, a symmetric NACA 0012 airfoil with a thickness-to-chord ratio of 12% was selected. The symmetric airfoil reduces adverse pitching moments and delays tip stall, which is particularly important for tailless flying-wing configurations where tip stall can lead to abrupt loss of control. A smooth S-curve interpolation was employed between the root and tip airfoils to ensure gradual variation of camber and thickness along the span.

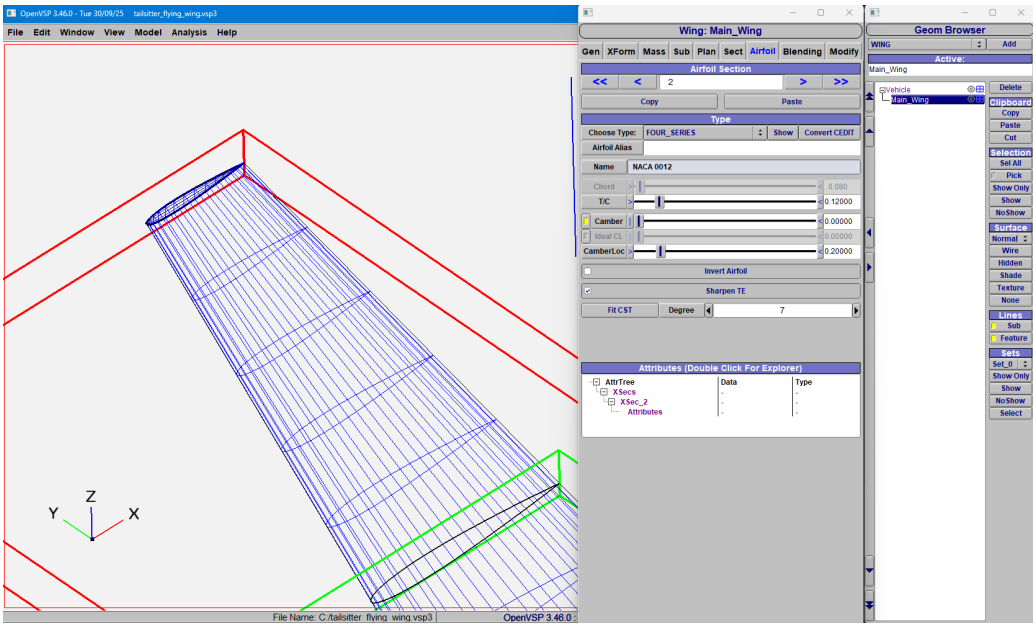

Figure 4: Wing Tip Airfoil Selection - NACA 0012

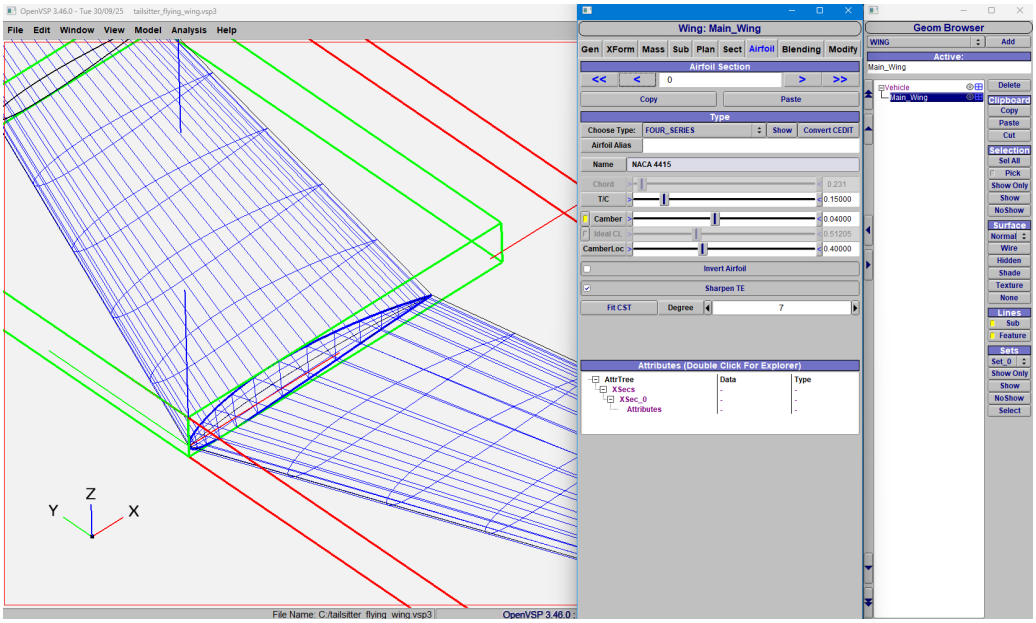

Figure 5: Wing Root Airfoil Selection - NACA 4415

4.3 Wing Twist (Washout)

A linear geometric washout was applied from the wing root to the wing tip:

- **Root Twist:** $0°$
- **Tip Twist:** $-2°$

This aerodynamic washout ensures that the local angle of attack at the wingtips is lower than at the root. Consequently, stall begins at the root and progresses outward. This preserves aileron (elevon) authority at the tips even as the main wing begins to stall, a safety-critical feature for the transition phase where angles of attack can be extreme.

5 Blended Center Body Implementation

Rather than introducing a separate fuselage, a blended center-body configuration was implemented by locally increasing the thickness of the central wing sections. Multiple wing sections were used to smoothly transition from the thickened center region to the baseline wing geometry. The maximum thickness in the center region was limited to approximately 18–20% of the local chord to avoid excessive aerodynamic penalties.

In OpenVSP, this was achieved by using multiple cross-sections with specific skinning controls to ensure continuity (C2 continuity). This blended region houses the flight controller, battery, and avionics. This design choice reduces the "wetted area" compared to a pod-and-boom configuration, directly contributing to the low drag coefficient observed in analysis.

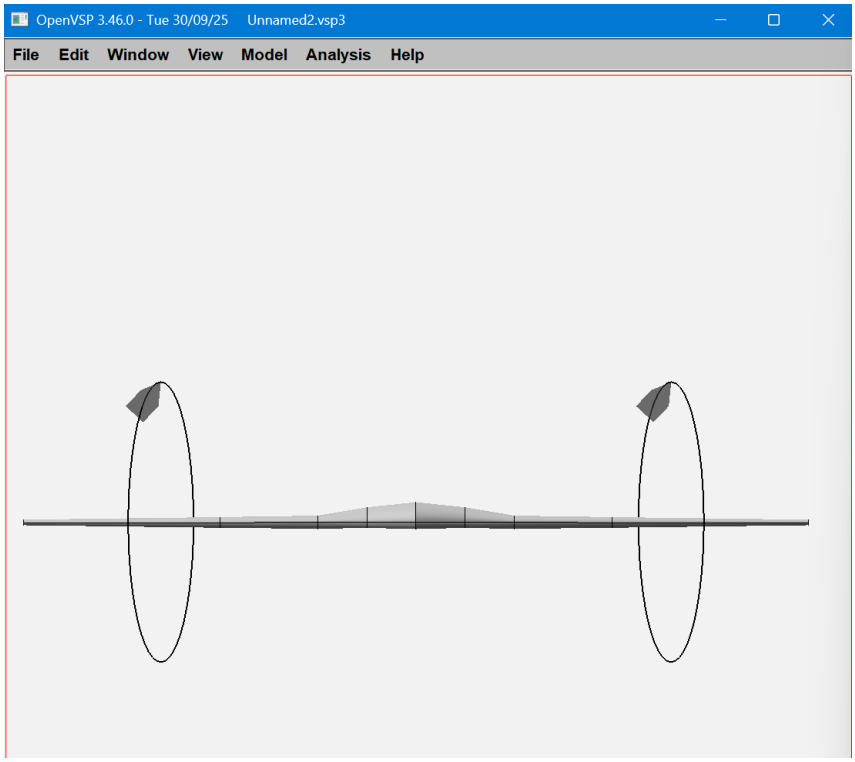

Figure 6: Blended center-body configuration achieved by locally increasing the thickness of the central wing sections.

6 Control Surfaces

The aircraft utilizes full-span control surfaces, specifically **elevons**, located on the outboard wing sections.

- **Function:** They mix pitch (elevator) and roll (aileron) control.
- **Sizing:** The elevons span approximately 60% to 80% of the semi-span with a chord ratio of 25%.
- **Placement:** They are positioned outboard to maximize the moment arm for roll control, but sufficiently immersed in the propeller slipstream to allow for vectoring of the thrust during hover.

The use of elevons is standard practice for tailless flying-wing configurations and provides sufficient control authority during both forward flight and transition phases.

7 Propulsion System Modeling

Twin wing-mounted tractor propulsion units were modeled using streamlined ellipsoidal nacelles to represent the motor housing and spinner. Each nacelle had a characteristic length of approximately 0.12 m and a maximum diameter of approximately 0.05 m. The nacelles were positioned near 25–35% of the semi-span to balance thrust distribution and structural considerations.

Propellers were represented using actuator disks with a diameter of approximately 0.27 m. This simplified representation avoids excessive geometric complexity while clearly defining thrust locations for aerodynamic and structural analysis.

The twin tractor configuration provides redundancy. In the event of a single motor failure, the aircraft can potentially enter a flat spin recovery or controlled descent, which is impossible with a single-engine tail-sitter.

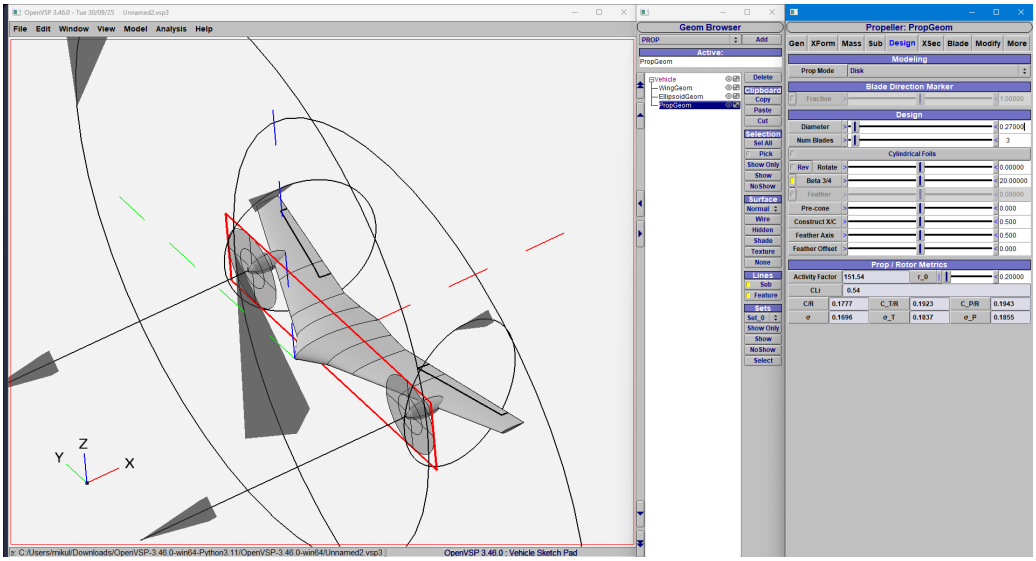

Figure 7: Ellipsoidal motor nacelles with actuator disk representation of the propellers in a twin tractor configuration.

8 Aerodynamic Analysis Using OpenVSP

This section documents the methodology, assumptions, solver settings, and results of the preliminary aerodynamic analysis conducted using OpenVSP. Two complementary approaches were employed:

- Parasite drag build-up analysis
- Panel-method aerodynamic analysis using VSPAERO.

Together, these methods provide a consistent conceptual-level assessment of the aerodynamic performance of the proposed tail-sitter UAV.

8.1 Parasite Drag Estimation

8.1.1 Methodology

Parasite drag was estimated using the built-in drag build-up method available in OpenVSP. This approach computes the zero-lift drag coefficient by summing contributions from skin-friction drag and form drag based on component wetted areas and empirical correlations. While this method does not capture induced drag or unsteady flow effects, it is widely used for conceptual design studies to obtain first-order drag estimates.

The analysis was conducted for a representative forward-flight cruise condition corresponding to low subsonic operation, consistent with the intended mission profile of the UAV.

8.1.2 Flight Condition and Atmospheric Assumptions

The following flight conditions were used for parasite drag estimation:

- **True airspeed:** 100 km/h (27.8 m/s)
- **Altitude:** 0 m (sea level)
- **Mach number:** 0.08
- **Atmospheric model:** Standard sea-level conditions

This flight condition was selected to ensure that compressibility effects are negligible and that the Reynolds number regime is representative of small UAV operation.

8.1.3 Reference Geometry Parameters

The reference quantities used in the drag calculation were derived from the OpenVSP geometry:

- **Wing planform area:** 0.22–0.24 m^2
- **Wetted area:** Automatically computed by OpenVSP
- **Reference length:** Mean Aerodynamic Chord (MAC)
- **MAC value:** 0.17 m

The mean aerodynamic chord was selected as the reference length because it provides a physically meaningful scale for non-dimensional aerodynamic coefficients for tapered flying-wing configurations.

8.1.4 Excrescence Drag Modeling

To account for real-world drag sources not explicitly modeled in the geometry, an excrescence drag increment was applied. These sources include:

- Surface roughness
- Control surface hinge gaps
- Manufacturing tolerances
- Small protuberances and junction imperfections

An excrescence increment of 7% was applied to the baseline parasite drag coefficient. This value is representative of a clean, small-scale UAV configuration and is commonly adopted in conceptual-level drag build-up analyses.

8.1.5 Parasite Drag Result

The resulting zero-lift drag coefficient including excrescence effects was found to be:

$$C_{D0} \approx 0.018 \tag{1}$$

This implies a highly efficient airframe. For comparison, a standard Cessna 172 has a C_{D0} of roughly 0.027, and many foam UAVs exceed 0.03. This low drag value suggests the blended body and clean wing design were successful strategies.

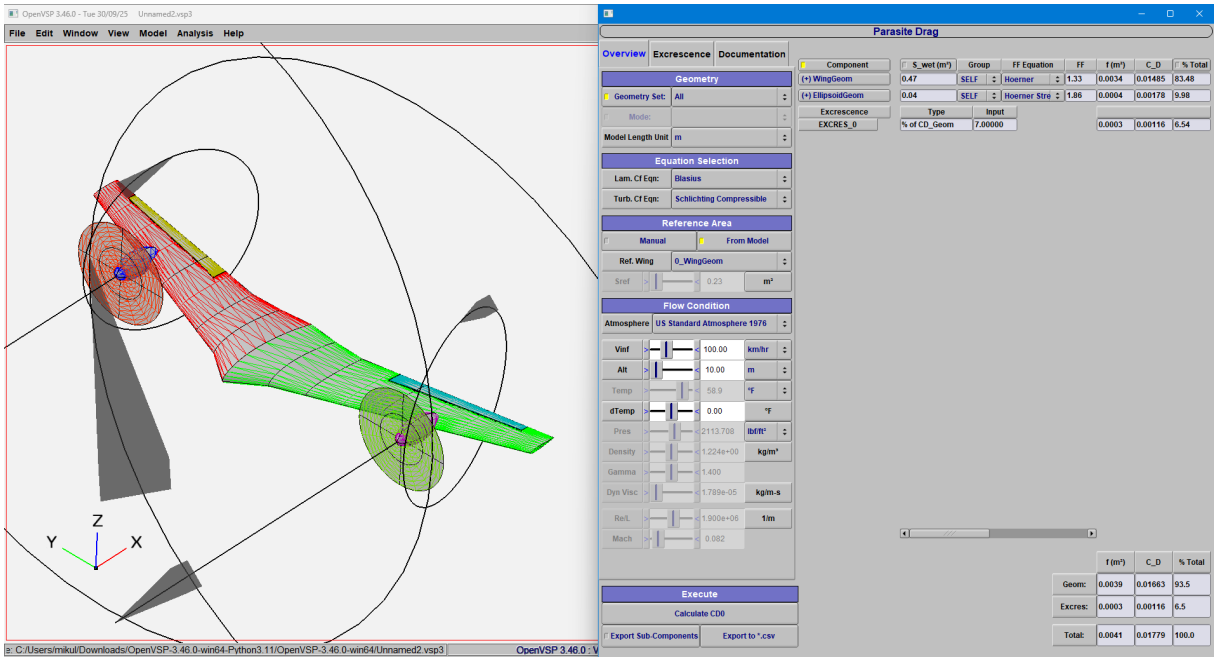

Figure 8: Parasite drag estimation using the OpenVSP drag build-up method at a cruise speed of 100 km/h with excrescence effects included.

8.2 Aerodynamic Analysis Using VSPAERO

8.2.1 Solver Description

VSPAERO is a vortex-lattice / panel-method solver integrated within OpenVSP. It computes aerodynamic forces and moments under the assumption of inviscid, irrotational flow. While viscous effects and flow separation are not explicitly captured, VSPAERO is well suited for evaluating lift, induced drag, and pitching moment trends within the pre-stall flight regime at the conceptual design stage.

8.2.2 Geometry and Symmetry Assumptions

The full aircraft geometry was modeled in OpenVSP, including the blended center body, elevons, motor nacelles, and propeller disks (represented geometrically only). No geometric symmetry was imposed in the solver to avoid inconsistencies between reference area definitions and force integration.

- **Symmetry:** Disabled
- **Half-model assumptions:** Not used

This approach ensures that all aerodynamic coefficients are computed based on the full aircraft geometry.

8.2.3 Reference Quantities and Coordinate System

To ensure physically meaningful aerodynamic coefficients, reference quantities were manually specified:

- **Reference area:** Wing planform area ($\approx$0.23 m^2)
- **Reference span:** $\approx$1.4m
- **Reference span:** $\approx$1.4m
- **Reference chord:** Mean Aerodynamic Chord (MAC $\approx$ 0.17 m)

The body-fixed coordinate system was defined such that:

- **X-axis:** Aligned with the forward-flight direction
- **Z-axis:** Positive upward (lift direction)
- **Y-axis:** Lateral direction

8.2.4 Angle-of-Attack Sweep Parameters

Angle-of-attack sweeps were conducted to evaluate lift, drag, and pitching moment behavior across the pre-stall flight envelope.

The sweep parameters were:

- **Angle-of-attack range:** 4° to $+14^\circ$
- **Increment:** 2°
- **Flight speed:** 25 m/s
- **Altitude:** Sea level

This range captures negative-lift conditions, cruise operation, and high-lift operation while remaining within the validity limits of panel-method analysis.

Lift and drag were projected along the Z and X axes, respectively. This definition is particularly important for tail-sitter configurations, where the aircraft orientation differs between hover and forward flight.

8.2.5 Airfoil Interpolation and Numerical Settings

To ensure smooth geometric variation and numerical stability:

- **Airfoil interpolation:** S-curve
- **Reference chord definition:** MAC (not CAVE)

- **Wake modeling:** Default steady wake
- **Solver type:** Steady-state

The S-curve interpolation ensures gradual variation of thickness and camber between the root (NACA 4415) and tip (NACA 0012) airfoils, which is particularly important given the locally thickened center-body region.

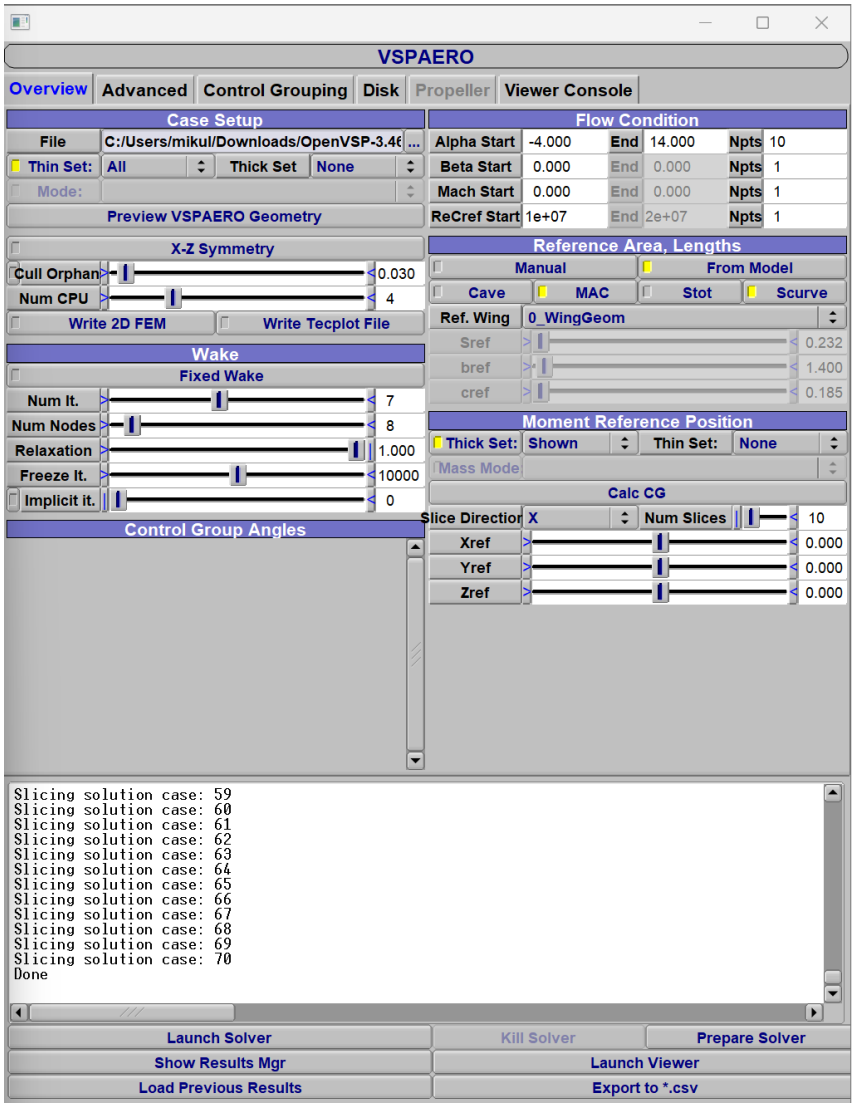

Figure 9: Parameters used for Aerodynamic Analysis

8.3 Aerodynamic Results and Discussion

8.3.1 Lift Characteristics

The lift coefficient exhibited an approximately linear variation with angle of attack within the analyzed range. At an angle of attack of 10°, the aircraft produced a lift coefficient of approximately:

$$C_L \approx 0.85 \tag{2}$$

This value is consistent with expectations for a moderately cambered flying-wing configuration operating at low Reynolds numbers. The applied washout and airfoil selection

contribute to maintaining lift generation without excessive pitching moment.

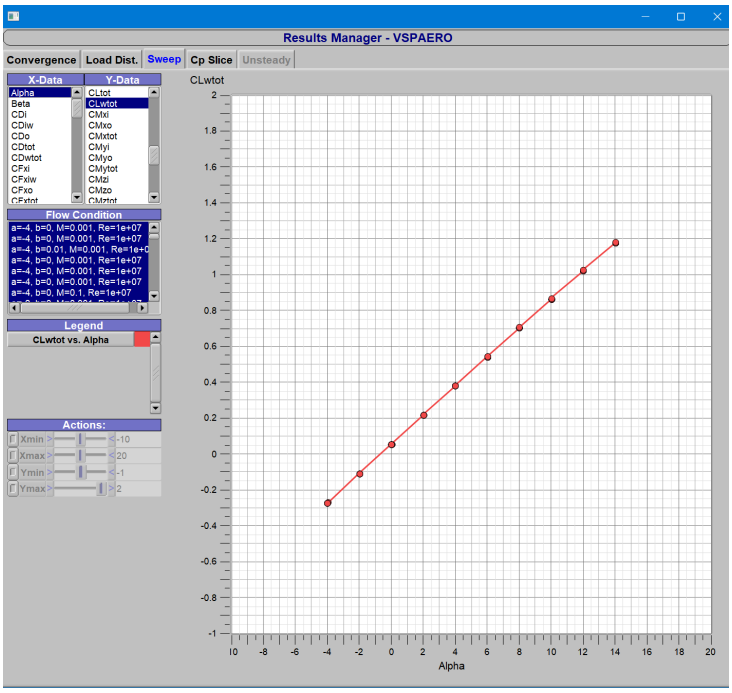

Figure 10: Lift coefficient variation with angle of attack

8.3.2 Drag Characteristics

The drag coefficient increased smoothly with angle of attack, reflecting the expected rise in induced drag as lift increases. When combined with the previously estimated parasite drag, the total drag behavior indicates good aerodynamic efficiency in the cruise and high-lift regimes.

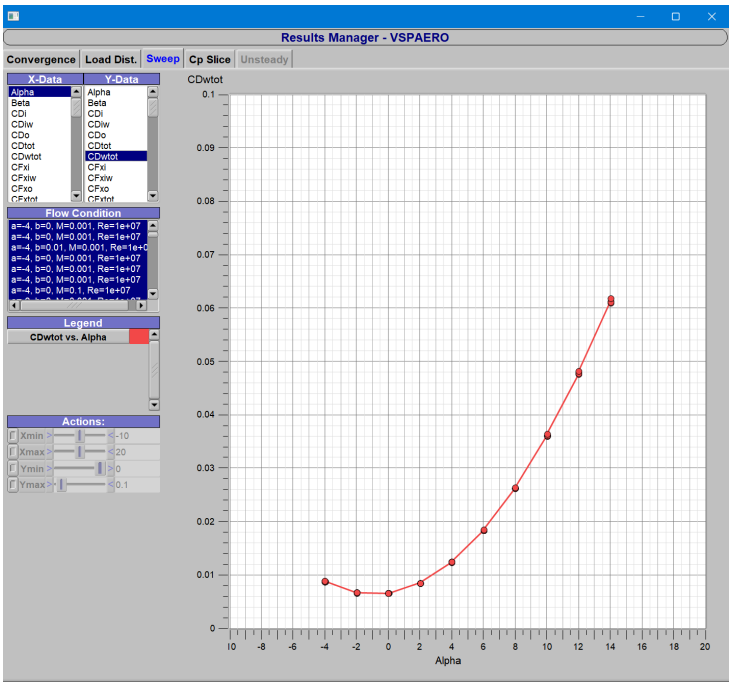

Figure 11: Drag coefficient variation with angle of attack

8.3.3 Aerodynamic Efficiency

The lift-to-drag ratio exhibited a clear maximum at moderate angles of attack, corresponding to the most aerodynamically efficient operating condition. This angle of attack was selected as the representative cruise condition for performance discussion.

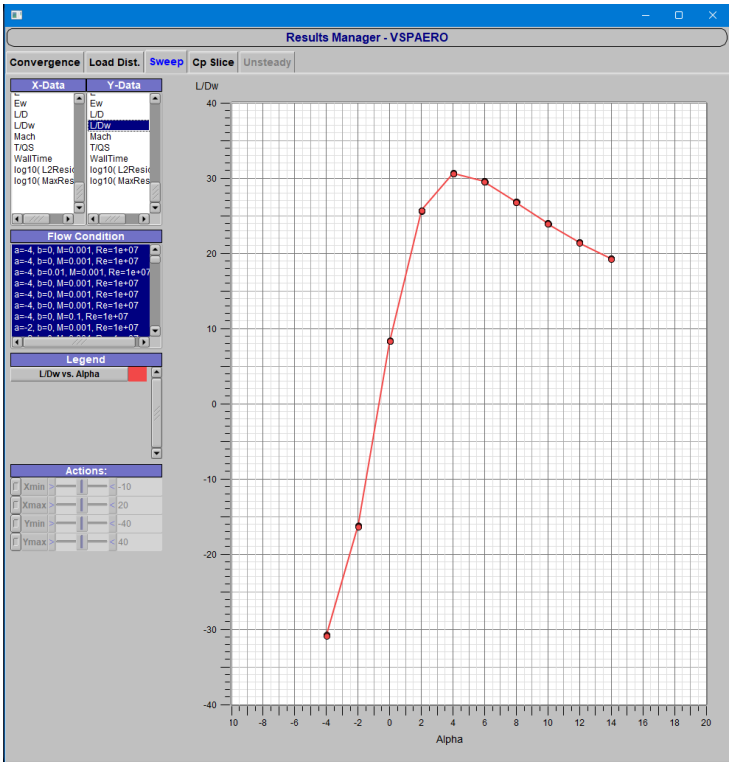

Figure 12: L/D ratio variation with angle of attack

8.4 Limitations of the Analysis

It is important to note that the aerodynamic analysis presented here is subject to the limitations of the employed methods. VSPAERO does not model viscous effects, flow separation, or propeller–airframe interaction. Consequently, the results are intended for conceptual design validation rather than high-fidelity prediction. These limitations motivate future studies using Reynolds-averaged Navier–Stokes (RANS) CFD and experimental validation.

9 Structural Analysis Considerations

Although the primary focus of this report is aerodynamic design, the geometry was created with structural constraints in mind.

- **Load Paths:** The straight leading edge of the internal structural box (spar location) allows for a continuous carbon fiber tube or I-beam spar.
- **Material:** The volume analysis from OpenVSP supports the use of expanded polypropylene (EPP) foam for the wing core, reinforced with carbon fiber spars, a standard method for lightweight UAVs.

- **FEM Compatibility:** The OpenVSP model was exported as an STL and STEP file, which verified that the geometry is "watertight" and suitable for meshing in Finite Element Analysis (FEA) software for future stress testing.

10 Conclusions

A conceptual design and preliminary aerodynamic analysis of a tail-sitter VTOL UAV based on a tailless flying-wing configuration was performed using OpenVSP and the VSPAERO panel-method solver. The aircraft geometry was developed parametrically, enabling systematic evaluation of wing planform parameters, airfoil selection, twist distribution, control surface integration, and propulsion layout.

The final configuration features a moderately high aspect ratio wing of approximately 9, with a wingspan of about 1.4 m and a wing planform area of approximately 0.22–0.24 m^2. A cambered NACA 4415 airfoil with a thickness-to-chord ratio of 15% was selected at the wing root to enhance lift generation and structural stiffness, while a symmetric NACA 0012 airfoil with a thickness-to-chord ratio of 12% was employed at the wing tip to improve stall behavior and reduce adverse pitching moments. A linear geometric washout of -2° from root to tip was applied to delay tip stall and improve controllability.

Parasite drag analysis conducted at a representative cruise speed of 100 km/h and sea-level conditions yielded a zero-lift drag coefficient of approximately $C_{D0} \approx 0.018$, including a 7% excrescence increment. VSPAERO analysis over an angle-of-attack range of -4° to $+14^\circ$ demonstrated near-linear lift characteristics within the pre-stall regime, with a lift coefficient of approximately $C_L \approx 0.85$ at 10° angle of attack. The drag coefficient increased smoothly with angle of attack, and the lift-to-drag ratio reached a maximum at moderate angles of attack, indicating an aerodynamically efficient cruise condition.

Overall, the results indicate that the proposed tail-sitter flying-wing UAV can achieve favorable aerodynamic performance while maintaining structural and mechanical simplicity. The developed configuration and analysis framework provide a solid foundation for subsequent structural analysis, higher-fidelity CFD studies, and flight dynamics and control investigations.

11 Future Work

To advance this project to a flight-ready prototype, the following steps are proposed:

1. **CFD Analysis:** Perform RANS (Reynolds-Averaged Navier-Stokes) CFD simulations to analyze high-angle-of-attack behavior (post-stall) during the transition phase, which VSPAERO cannot accurately predict.
2. **Structural Sizing:** Detailed FEM analysis to size the main spar for the high bending moments experienced during a 3G pull-up maneuver.
3. **Propulsion Testing:** Static thrust stand testing of selected motor-propeller combinations to validate efficiency assumptions.
4. **Control Law Development:** Simulation of the transition maneuver (hover to forward flight) to tune PID gains for the flight controller.